TEXTURAL VARIATIONS AND CHEMICAL MOBILITY DURING MYLONITIZATION: THE EL TIGRE GRANITOID SHEAR ZONE, SIERRA DE PIE DE PALO, WESTERN SIERRAS PAMPEANAS, SAN JUAN

Brígida CASTRO DE MACHUCA[1,2], Diego MORATA[3], Sandra PONTORIERO[1] y Gloria ARANCIBIA[4]

[1] Instituto de Geología (INGEO) - Departamentos de Geofísica y Geología, FCEFN, Universidad Nacional de San Juan.
[2] CONICET. Email: bcastro@unsj-cuim.edu.ar.
[3] Departamento de Geología, Universidad de Chile, Santiago, Chile. Email: dmorata@cec.uchile.cl.
[4] Departamento de Ingeniería Estructural y Geotécnica Pontificia. Universidad Católica de Chile, Santiago, Chile. Email: garancibia@ing.puc.cl

ABSTRACT. A high-strain ductile shear zone trending NEE with southeasterly dipping mylonitic foliation, has been recognized affecting a Mesoproterozoic (*ca.* 1105 Ma) peraluminous garnet-bearing two mica granitoid (El Tigre granitoid: 31º31'30"S-68º15'12"W) which is part of the crystalline basement of the Sierra de Pie de Palo, Western Sierras Pampeanas. Kinematic analysis indicates a main strike-slip component and provides evidence that the relative movement within the shear zone have dextral sense. Relict igneous and peak amphibolite facies metamorphic mineral assemblages and textures are preserved in the granitoid protolith although, within the shear zone, deformation obliterates those generating typical mylonitic fabrics. Mylonitization operated under open-system conditions, provoking mobilitization (either enrichment or depletion) of almost all major and trace elements, including rare earth elements and Rb/Sr and Sm/Nd isotopes. Observed chemical variations are mostly controlled by syntectonic fluid-transport processes and decrease in the garnet, biotite and accessory minerals amounts during mylonitization, and the neoformation of white-mica in the fine-grained mylonite matrix. Moreover, the different isotopic signatures between the protolith and the mylonites could be a consequence of mechanisms of deformation-driven processes assisted by fluid flow with different fluid-host rock interaction ratios. Textural, modal and chemical changes between the El Tigre granitoid protolith and its mylonites, allow reconstructing its tectono-metamorphic evolution and the metamorphic conditions achieved. Paragenetic associations and deformation textures on mylonites suggest that El Tigre granitoid shear zone was developed under low-T greenschist facies conditions, probably at temperatures below 400 °C. This deformational event took place at *ca.* 473 ± 10 Ma during the Famatinian orogeny.

Keywords: *Ductile shear zone, Granitoid mylonites, Microstructures, Geochemical mobility, Greenschist facies.*

RESUMEN: *Variaciones texturales y movilidad geoquímica asociadas a milonitización: la zona de cizalla del granitoide El Tigre, Sierra de Pie de Palo, Sierras Pampeanas Occidentales, San Juan*. Una faja de cizalla dúctil con foliación milonítica de dirección NEE y buzamiento al sudeste, afecta a un granitoide mesoproterozoico (Granitoide El Tigre: 31º31'30"S-68º15'12"O) que forma parte del basamento cristalino de la Sierra de Pie de Palo, Sierras Pampeanas Occidentales. El análisis cinemático de la faja indica una componente principal de desplazamiento de rumbo con sentido de movimiento dextral. En el granitoide no deformado (protolito) se preservan asociaciones minerales y texturas relícticas, ígneas y metamórficas, que son obliteradas por la deformación. La milonitización operó en un sistema abierto provocando la movilización (ganancia o pérdida) de casi todos los elementos mayores y traza, incluyendo las tierras raras e isótopos de Rb/Sr y Sm/Nd. Los cambios químicos fueron controlados mayormente por transporte sintectónico de fluidos y por transformaciones mineralógicas producidas durante la milonitización (disminución del contenido de granate, biotita y minerales accesorios y neoformación de mica blanca en la matriz de las milonitas). Las variaciones isotópicas entre el protolito y las milonitas también serían resultado de la intervención de fluidos durante la deformación, con interacción variable entre fluido y rocas de caja. Los cambios texturales, mineralógicos y químicos experimentados por el granitoide durante la milonitización, permiten reconstruir su evolución tectono-metamórfica y las condiciones metamórficas imperantes. Las asociaciones minerales y microestructuras de deformación de las milonitas sugieren para la faja de cizalla del granitoide El Tigre condiciones propias de la facies de esquistos verdes, con temperaturas inferiores a los 400 °C. Este evento deformante tuvo lugar a los 473 ± 10 Ma durante la orogenia Famatiniana.

Palabras clave: *Zona de cizalla dúctil, Milonitas de granitoide, Microestructuras, Movilidad geoquímica, Facies de esquistos verdes.*

INTRODUCTION

Mechanical processes leading to the development of mylonites are strongly dependent on the modal mineralogy (bulk composition), heterogeneity of the rock, and temperature and pressure conditions during deformation. The chemical and isotopic evolutions of mylonites are much more complex processes not well understanding yet. As several authors pointed out (*e.g.* Sinha *et al.* 1986 and references therein) the mobility of chemical elements in shear zones will depend on a number of variables, mainly the mineralogical/chemical composition and texture of the protolith as well as the deformation regime. Most shear zones are characterized by the availability of fluids, the presence of a fluid phase during deformation enhances solution transport, microfracturing and recrystallization and generates new mineral assemblages replacing or in addition to the relict mineral assemblage.

A well exposed low-grade ductile shear zone and related mylonites has been recognized at the El Tigre creek, southwest Sierra de Pie de Palo, San Juan province (Fig. 1). This exhumed shear zone offers a good opportunity to examine the interaction of deformation processes and textural and compositional changes involving a Mesoproterozoic (*ca.* 1105 Ma U-Pb SHRIMP zircon age, Morata *et al.* 2010) peraluminous garnet-bearing two mica granitoid (El Tigre granitoid) in its original tectonic setting.

Petrographic variations and the behavior of elements and isotopic signatures experienced by the El Tigre granitoid during mylonitization are here presented. Sampling was developed from centimeter-scale mylonite bands and neighboring granitoid protolith, covering the entire strain-gradient fabric from undeformed/slightly deformed protolith to mylonite-ultramylonite. The coupled microstructural and geochemical (major, trace elements and Rb/Sr-Sm/Nd isotopes) investigations allow us to link specific geochemical and mineralogical changes to particular microstructural changes. Previously obtained deformation age (473 ± 10 Ma K-Ar age on recrystallized micaceous matrix, Castro de Machuca *et al.* 2008, Morata *et. al.* 2010) also allows to constrain the deformational event and reconstruct its tectono-metamorphic evolution.

GEOLOGIC SETTING

The Sierra de Pie de Palo, Western Sierras Pampeanas, considered to represent part of the Proterozoic basement of the Precordillera terrane (Astini *et al.* 1995, Casquet *et al.* 2001, Thomas and Astini 1996), is characterized by a complex polyphase tectono-metamorphic history. It is a supposed exotic block of Laurentia rifted away in Late Neoproterozoic-Early Cambrian times, and accreted to the proto-Andean margin of Gondwana during the Famatinian orogeny (Mid-Ordovician), although its allochthonous character has been seriously questioned by Finney *et al.* (2003) and Galindo *et al.* (2004). The time of collision of the Precordillera (Cuyania) terrane with Gondwana is tracked by the cessation of arc-related magmatic activity in the Gondwana protomargin, at about 465 Ma (*e.g.* Rapela *et al.* 2001, Baldo *et al.* 2001, Casquet *et al.* 2001, Vujovich *et al.* 2004). Nevertheless, deformation continued through most of the Early Paleozoic until amalgamation of the Chilenia terrane by the Late Devonian.

The Sierra de Pie de Palo is composed of a metamorphic basement with two different sequences (Fig. 1): the Pie de Palo Complex (Ramos and Vujovich 2000) characterized by augen orthogneisses, biotite-muscovite-garnet gneisses, schists, amphibolites and ultramafic rocks of Mesoproterozoic (Grenvillian) age (*e.g.* Pankhurst and Rapela 1998 and references therein), mostly derived from island arc and oceanic environments, and the Caucete Group (Ramos and Vujovich 2000), characterized by a platform siliciclastic to carbonate sequence of Late Cambrian age (Galindo *et al.* 2004). Relationships between both complexes are always structural where exposed. Included in the Pie de Palo Complex, Galindo *et al.* (2004) differentiate the Neoproterozoic (580-720 Ma) Difunta Correa meta-sedimentary sequence, considered a cover to the rejuvenated Grenvillian basement. Granitoid rocks of diverse nature and age (amongst which is the El Tigre granitoid) make up only a small proportion of the crystalline basement of the Sierra de Pie de Palo. Granitoids are found intruding the Middle to Late Proterozoic sequences.

According to Casquet *et al.* (2001) two different metamorphic events were registered in the Sierra de Pie de Palo; a low P/T type metamorphism reaching in some places migmatitic conditions and a later Famatinian metamorphism under higher P/T conditions, following a clockwise P-T path.

Structurally, the Sierra de Pie de Palo is an imbricate ductile thrust system with a top-to-the-west sense of relative movement, uplifted on the Pliocene-Quaternary (Ramos and Vujovich 2000). Along the western flank of the Sierra de Pie de Palo, the Las Pirquitas thrust, a NNE trending ductile shear zone (Fig. 1), is considered as a major high-strain low-angle thrust that places the Pie de Palo Complex over the Caucete Group (Vujovich and Ramos 1994, Ramos *et al.* 1996 and references therein). The Las Pirquitas thrust has closely associated subsidiary thrust top-to-the-west related shear zones (Mulcahy *et al.* 2004, Vujovich *et al.* 2004).

THE EL TIGRE GRANITOID AND ITS MYLONITES: FIELD OCCURRENCE, PETROGRAPHY AND MICROSTRUCTURES

The El Tigre granitoid and mylonites-ultramylonites derived from it, crop out near the downstream of the El Tigre creek (31°31'30"S-68°15'12"W) on the southwestern end of the Sierra de Pie de Palo, about 30 km east from San Juan city (Fig. 1).

The El Tigre granitoid is represented by tabular to lenticular vein-like bodies (Fig. 2 a-b) that range from few centimeters to some few meters in wide, distributed in a small area on both sides of the El Tigre creek. It intrudes concordantly the schistosity of the host rocks of the Pie de Palo Complex, which locally consist of quartz-muscovite and quartz-plagioclase-biotite-muscovite±garnet mylonite schists.

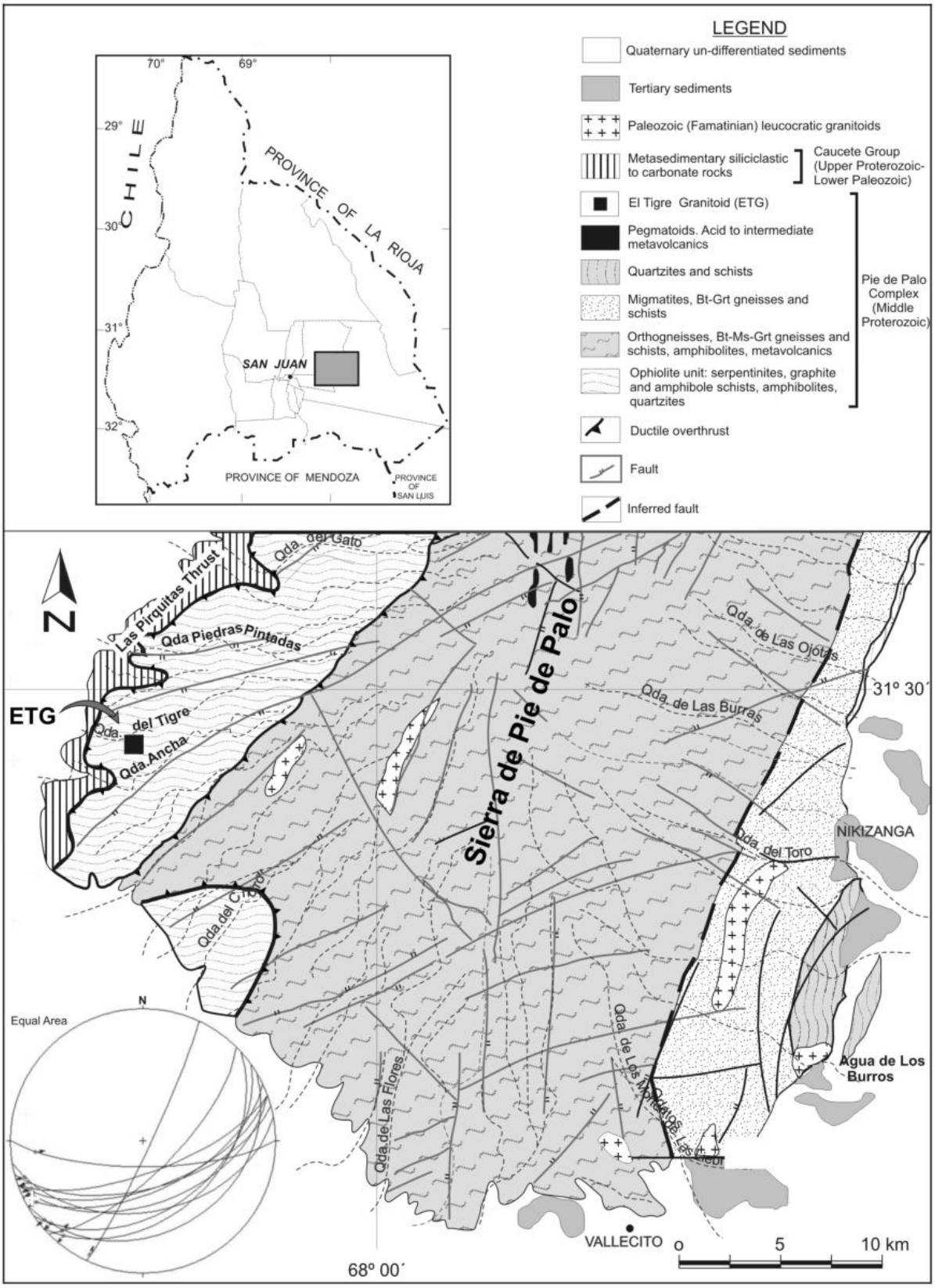

Figure 1: Schematic geologic map of southern Sierra de Pie de Palo, Western Sierras Pampeanas, San Juan province, showing the locality (ETG) where the data and samples were obtained (adapted from Ramos and Vujovich 2000 and Naipauer *et al.* 2005). Inset shows stereonet plot of mylonitic foliation and pitch of the El Tigre granitoid shear zone (N = 12).

The El Tigre granitoid is folded together with the country rocks and, due to rheology contrast, *boudinage* is frequently developed. The tectonic analysis of the El Tigre creek and its surroundings reveals superposition of at least three deformational events as previously noticed by Dalla Salda and Varela (1982), Castro de Machuca (1984) and Ramos and Vujovich (2000). The oldest one is represented by mesoscopic folds and axial-planar foliations trending approximately N75°E; the second one with an average direction N30ºW is the higher temperature event (amphibolite facies), meanwhile the third tectonic episode is locally represented by narrow shear zones. The El Tigre granitoid records post-intrusive deformation along these ductile shear zones developing a strong mylonitic foliation.

Local El Tigre granitoid ductile shear zones trending NEE (N25º-90°E) (see stereonet plot in Fig. 1) with moderate southeasterly dips, range from few centimeters to a meter wide. They are characterized by the presence of mylonites, stretching lineations and retrogressive mineral assemblages. Numerous microstructures, most of which are visible in the field as well as in thin sections, have been recognized and applied as kinematic indicators, amongst them are: mica-fish, pressure shadows, σ-type porphyroclasts, asymmetrical microfolds and microsheared feldspar porphyroclasts (bookshelf structure). Sometimes composite foliation planes (S-C' planes) develop simultaneously within the shear zone. The well developed kinematic markers in oriented samples of these mylonites and the prominent subhorizontal quartz stretching lineation (average pitch 10ºSW) (see stereonet plot in Fig. 1), indicate a main strike-slip component and provide evidence that the relative movement within the shear zone have dextral sense, with a minor component of normal displacement compatible with NWW shortening. This is consistent with kinematic observations registered along the Las Pirquitas thrust main shear zone and other ductile deformation zones in the area (*e.g.* Ramos *et al.* 1998, Vujovich *et al.* 2004, Mulcahy *et al.* 2004, 2005, 2007), collectively forming a network.

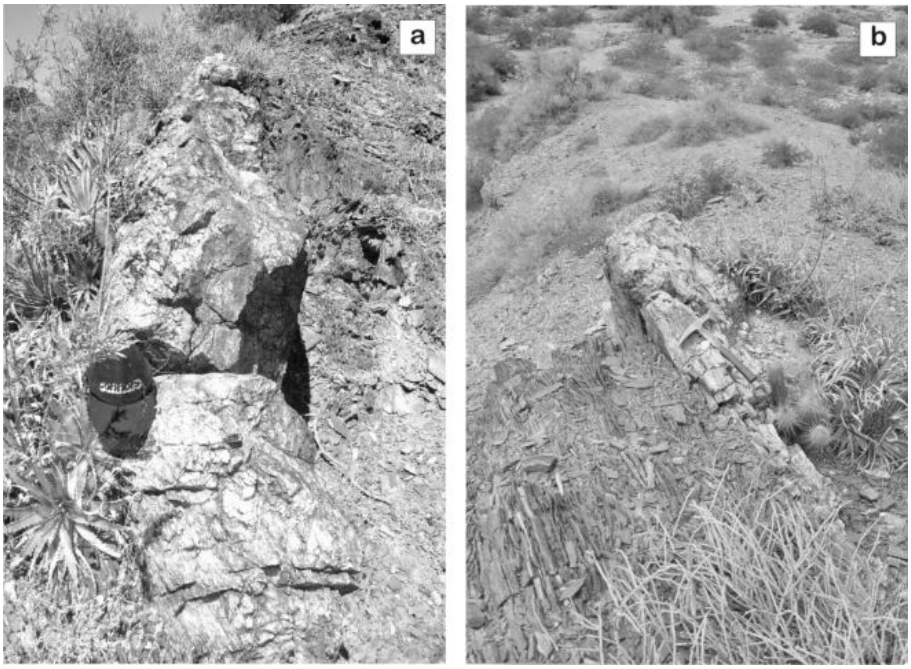

Figure 2: (a)-(b) Outcrop views of the El Tigre granitoid (ETG). Tabular to lenticular vein-like bodies intruded concordantly with the schistosity of the host rocks (quartz-muscovite schists) of the Pie de Palo Complex. Sharp contacts are observed.

From small-scale mylonite bands, the El Tigre granitoid is progressively transformed and grade laterally into several textural/compositional categories. To study petrographic, chemical and isotopic variations, sampling was developed covering the entire strain-gradient fabric from undeformed/slightly deformed protolith through moderately deformed granitoid to fine-laminated mylonite-ultramylonite (Fig. 3 a-e).

Undeformed/slightly deformed El Tigre granitoid (protolith)

The El Tigre granitoid protolith is a non-foliated medium-grained (3-5 mm grain size), light yellowish-gray colored, equigranular rock (Fig. 3 a-b). Variations on modal proportions (it fluctuates from granodiorite to tonalite) are due to primary magmatic compositional variations. Its granoblastic texture resembles that of the original intrusive rock. It is composed of plagioclase (An_{13-27}), quartz, microperthitic K-feldspar (in the granodioritic varieties), foxy-red biotite and muscovite (Ms1), with accessory garnet, zircon, rutile, monazite, and lesser allanite and ilmenite (Fig. 4a). Clinozoisite/zoisite and sericite are present as retrograde minerals. Biotite occasionally shows replacement by later muscovite (Ms_2) and chlorite along parting planes and edges. K-feldspar grains are occasionally rimmed by myrmekite and rarer muscovite- quartz symplectites are also found. Scarce chlorite and calcite veinlets are also observed.

Textural and mineralogical evidences suggest that after igneous crystallization the El Tigre granitoid underwent regional metamorphism (peak amphibolite facies) slightly obliterating primary igneous textures (Morata *et al.* 2008). Strain effects in the protolith are minor: some bending in micas, undulose extinction in quartz and limited subgrain formation with no recrystallization. Feldspars show no evidence of internal strain.

Moderately deformed granitoid

In the moderately deformed rocks, boundaries between feldspars grains are serrated and irregular. Micas are easily bent and notorious kinking is developed, quartz behaves plastically by various dislocation/glide mechanisms as undulose extinction and deformation lamellae. Progressive subgrain

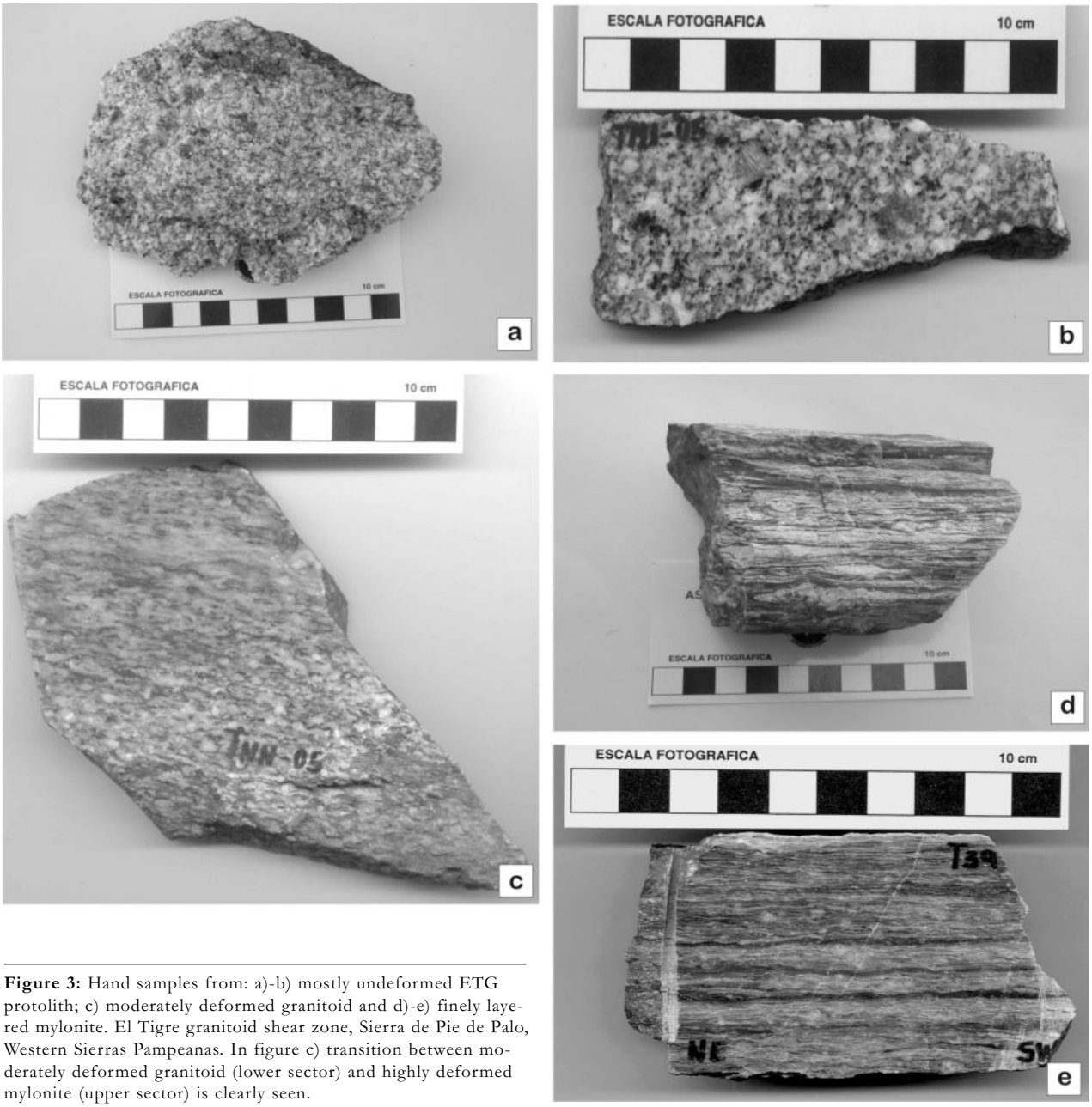

Figure 3: Hand samples from: a)-b) mostly undeformed ETG protolith; c) moderately deformed granitoid and d)-e) finely layered mylonite. El Tigre granitoid shear zone, Sierra de Pie de Palo, Western Sierras Pampeanas. In figure c) transition between moderately deformed granitoid (lower sector) and highly deformed mylonite (upper sector) is clearly seen.

development and incipient recrystallization especially at their boundaries (Fig. 4b) resulted in an incipient grain size reduction and grain boundary bulging.

Granitoid mylonites

Pronounced foliation and extensive grain-size reduction compared to the crystal size of the protolith, characterize the more-intense mylonitic deformation.

The El Tigre granitoid mylonites/ultramylonites are cohesive, strongly foliated and lineated rocks (Fig. 3 d-e) with up to 40% of feldspar porphyroclasts (maximum size 4.3 mm) and, more rarely, polycrystalline quartz porphyroclasts, in a very fine-grained (≤0.002 mm) foliated groundmass of dynamically recrystallized quartz, phyllosilicates and epidote (Fig. 4 c-d).

Feldspar porphyroclasts tend to be elliptical in shape with strong evidence of fracturing and slipping on crystallographic cleavage planes. Plagioclase shows evidence of brittle deformation by an *en-echelon* slip cleavage (bookshelf structure, Fig. 4 e-f). Feldspars behaved passively during shearing of the matrix, so they usually developed σ-type and pressure-shadow structures composed of quartz, epidote and fine-grained white mica. Undulose extinction, bending and deformation twins are common both in plagioclase (Fig. 4g) as well as in microcline porphyroclasts. Deformation twins in plagioclase vary from straight, to kinked, to poorly conserved. Although cross-hatched twinning is also

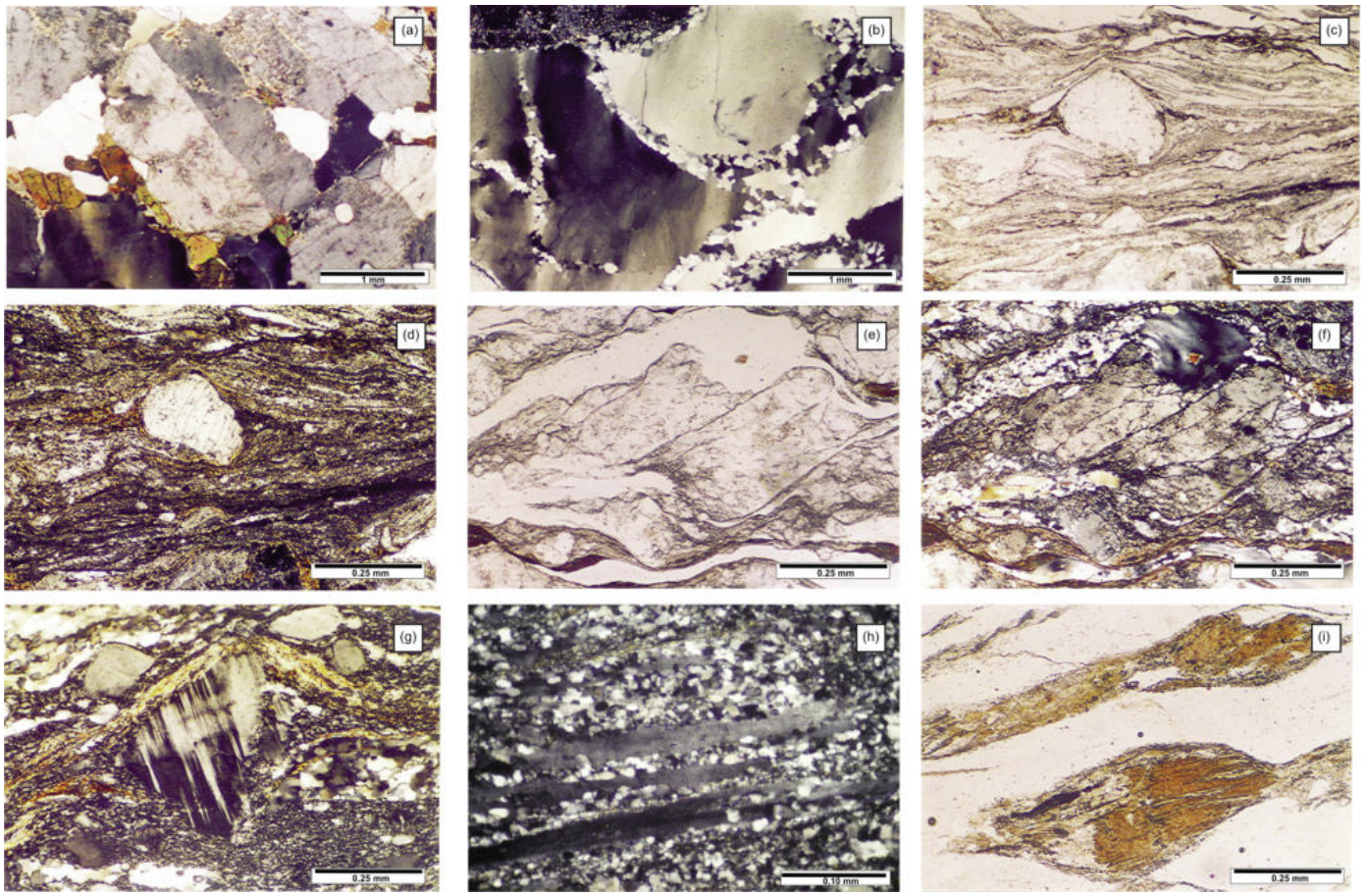

Figure 4: Textures and mineralogy of: a) the ETG granitoid protolith; b) moderately-sheared granitoid and c) to i) granitoid mylonites, Sierra de Pie de Palo, Western Sierras Pampeanas. a) Carlsbad twinned slightly sericitized subhedral plagioclase, strained quartz and biotite flakes (XPL); b) Large subgrained quartz grains with incipient recrystallization especially at their boundaries (XPL); c)-d) Plagioclase porphyroclasts in a very fine-grained well foliated quartz-phyllosilicates-epidote matrix (PPL-XPL); e)-f) Broken feldspar grain smeared out along shear planes (bookshelf structure) is in between finely recrystallized quartz (upper section) and quartz "ribbons" + ultra-fine-grained sericite (lower section). In the upper right corner, relict quartz grain shows strong undulose extinction (PPL-XPL); g) Single feldspars and polycrystalline quartz porphyroclasts around which mylonitic foliation is deflected. Deformation twins with tapered ends are seen in a plagioclase porphyroclast (centre) (XPL), (h) Mylonitic layering with alternance of finely recrystallized quartz and quartz "ribbons" produced by plastic deformation under high differential stress (XPL); i) Trails and stair-stepping between mica-fish (biotite) (PPL). PPL: plane-polarized light, XPL: cross-polarized light. In photomicrographs a)-b) scale bar is 1 mm, in photomicrographs c)-i) is 0.25 mm and in photomicrograph h) is 0.10 mm.

present, most microcline grains show deformation-enhanced twinning. Plagioclase is very often albitizied and partially transformed to sericite + epidote.

When polycrystalline quartz porphyroclasts are present, they show strong undulose extinction, sutured boundaries, and become progressively flattened defining foliation and lineation. The plastic deformation of quartz results in extremely long and thin ribbons, which are often partially to fully replaced by a very fine-grained mass of new recrystallized granoblastic to micropolygonal quartz aggregate (Fig. 4h). The widespread development of recrystallized quartz is one of the most prominent features in these mylonites. Very rare original quartz grains elongated parallel to the shear zone fabric are still present. In hand samples, the quartz ribbons show a characteristic blue tint.

Mica flakes develop characteristic mica-fish (Fig. 4i). Micas are severely bent and smeared out along foliation planes, multiplication of mica-fish by break-up and dispersion is common. Primary muscovite (Ms_1 + Ms_2) is shredded producing thin and very fine-grained layers of mica debris. Brittle garnet porphyroclasts are completely dismembered in small grain trails, and are no longer recognizable in the ultramylonites. With strain increasing, destruction of feldspar and micas is accompanied by a small but marked greater abundance of fine-grained muscovite and epidote-group minerals (zoisite/clinozoisite). New phyllosilicate and epidote grains are oriented by shearing as part of the matrix and individual grains show no evidence of intracrystalline deformation at the optical microscope scale. Deformation mechanisms in quartz range from subgrain rotation- to grain boundary migration recrystallization (GBMR). Deformation microstructures in feldspars include mainly: 1) microfracturing and

bookshelf, 2) deformation twins, 3) undulose extinction, 4) development of flame perthites and 5) development of deformation-induced myrmekites. Process 1) is more efficient at low to moderate strain, while 2) to 5) are active throughout the whole deformation history and dominant at large strain. Observed microstructures and deformation mechanisms at the El Tigre granitoid shear zone are consistent with those developed in low-grade greenschist facies conditions at *ca.* 300-400 °C (Passchier and Trouw 1996).

MINERALOGICAL CHANGES AND CHEMICAL MOBILITY DURING MYLONITIZATION

Mineralogical changes

Mylonitization in the El Tigre granitoid shear zone is characterized not only by the development of shear surfaces and strong grain size reduction but also by a significant change of modal and chemical compositions between the protolith and its mylonitic products. With increasing deformation across the mylonite zone, the protolith undergoes substantial changes in modal proportions (Table 1). Modes were obtained by conventional point counting (1100 points for each thin section) under an optical polarized microscope. In the case of mylonites, precise identification of matrix minerals was partly obstructed due to their fine grain size (≤ 0.002 mm).

Main mineralogical changes that occur from low-to high-strain zones include a drastic decreasing in the accessory minerals amounts (including garnet), as well as a notable increase in neoformed white-mica (sericite) and epidote group minerals during mylonitization (Table 1). Microperthitic K-feldspar experienced incipient to total replacement by microcline. From the protolith to mylonite, the total modal content of biotite decreases from *ca.* 8.1% to 5.3% while white mica (including original muscovite and fine-grained sericite) grows drastically from *ca.* 2.9% to 16.7%. Plagioclase contents decrease significantly with respect to the protolith (~ 50%) whereas the K-feldspar content shows a notable increase from *ca.* 4.7% to 11.2%. No significant variation is observed for quartz. Epidote content is irrelevant in the protolith but reaches up to 6.7% in mylonitic samples. The sum of modal contents for accessory minerals (including garnet) in the protolith is ~ 1.4% and decreases roughly to ~ 0.3 % in the mylonites. In addition to the relict igneous + metamorphic protomineralogy, the mylonites have a significant metamorphic mineralogy associated with the low- temperature ductile deformation event. With increasing strain, destruction of feldspars and micas is accompanied by a marked greater abundance of fine-grained white-mica (sericite) and epidote (mainly zoisite)-group minerals and hence water content of the total rock. Thus, the mineral assemblage characteristic of these mylonites implies addition of a fluid phase. Chloritization of biotite, growth of chequered albite, and flame perthite, are also relevant changes.

The replacement of the load bearing framework silicates by an intrinsically weaker fine-grained phyllosilicate aggregate is an important process; dynamic recrystallization enabled the mineral reactions which produced the rheologically softer minerals.

TABLE 1: Average modal mineral analyses of representative samples from the El Tigre granitoid protolith and its mylonites by point counting of thin sections (n = 1100). Counts per sample expressed as a percentage.

Characteristics	Microstructural Type	
Rock type	Undeformed/slightly deformed ETG	Mylonite-Ultramylonite
Relative strain	Low	Very high
Samples	S4S, S15S, S27	S1S, T39, TM7-0,5
Mineralogy	**Average Modal Proportion (%)**	
Quartz	32.4	34.6
Plagioclase	50.5	25.0
K-Feldspar	4.7	11.2
Biotite	8.1	5.3
Muscovite	2.9	16.7*
Garnet	0.8	0.1
Accessory minerals	0.6	0.3
Epidote group minerals	---	6.7
Total:	100%	99.9%

* includes mostly fine-grained white mica (sericite)

Chemical mobility

In order to understand chemical changes that may have occurred during mylonitization of the El Tigre granitoid as a function of strain and associated hydration, thirteen whole-rock analyses were made on undeformed/slightly deformed protolith (samples S4S, S15, S15S, S27 and TM1-05), moderately deformed (samples S21, TM3-05 and TM6-05) and highly deformed mylonites (samples TM4-05, S1S, T39, TM2-05 and TM7-05). Samples were analyzed at the ALS Chemex Laboratories (Vancouver, Canada). Major elements were determined by standard X-ray fluorescence spectrometry, and trace elements including rare earth elements (REE) by inductively coupled plasma mass spectrometry (ICP-MS). Instrumental uncertainties are as follow: all major elements ± 0.01%; Cs, Ho, Lu, Tb, Tm ± 0.01 ppm; Er, Eu, Sm, Yb ± 0.03 ppm; Dy, Gd, Th, U ± 0.05 ppm; Ga, Nd, Sr, Ta ± 0.1 ppm; Hf, Nb, Rb ± 0.2 ppm; Ba, Ce, Co, La, Y, Zr ± 0.5 ppm; Cu, Ni, Pb, V, Zn ± 5 ppm; Cr ± 10 ppm. The data are shown in Table 2.

Mobility of chemical elements in ductile shear zones depends mainly on the mineralogy, texture and chemical composition of the protolith, as well as the deformation regime. Chemical data can be used to gain insight into the nature of the metasomatic processes that operated during mylonitic deformation. The isocon method of Grant (1986) using Gresens' technique was applied to assess the apparent mobility of elements within the El Tigre granitoid shear zone. To plot chemical variations on the isocon diagrams (Fig. 5), the composition of the least deformed and hence more representative sample of the protolith (sample TM1-05) has been selected as the reference composition. All element concentrations (multiplied by different scaling factors) are plotted on a protolith vs. mylonite rock (*e.g.* sample TM7-05) diagram. Those elements plotting in a same straight line passing by the origin would define an isocon. If no volume change was occurred, this line would

have a 1:1 ratio and elements systematically plotting over and under this constant mass isocon would be gained or lost to the system, respectively.

Regarding geochemical changes, mylonitization at the El Tigre granitoid shear zone operated under open-system conditions, provoking mobilitization (either enrichment or depletion) of almost all major and trace elements, including rare earth elements and Rb/Sr and Sm/Nd isotopes.

Average analysis from typical mylonites (samples S1S, T39, TM2-05 and TM7-05), compared to average analysis of undeformed granitoid (samples S4S, S15, S15S, S27 and TM1-05), shows gain of K_2O (~ 8%, exceptionally up to 31% in sample TM7-05 and 53% in sample T39) and significant losses of P_2O_5 (~ 25%), CaO (~ 35%) and MnO (~ 37%), while other elements change more drastically, *e.g.* total Fe (~ 41%), TiO_2 (~ 48%) and MgO (~ 51%). Since mylonite sample T39 is derived from a potassium feldspar-rich protolith, the high K_2O content would not only be attributed to geochemical mobilization. Al_2O_3, Na_2O and SiO_2, behave as almost immobile during mylonitization; they only show irrelevant (< 5%) decreasing or increasing compared to the protolith. Moderately deformed rocks are transitional between these extreme-rock types and also show intermediate chemical compositions.

The element mobility is mainly a function of the amount of relict, recrystallized and neocrystallized minerals. Thus, decrease in Fe, Mg and Ti could be mainly related to the destruction of biotite during mylonitization. Also losses in Fe, Mg, Mn and Ti are probably due to replacement and/or disappearance of ilmenite, rutile and garnet. A notable increase (~ 15%) in loss on ignition (LOI $\approx$ H_2O) during mylonitization progress is also observed due to the increase in newly formed hydrous minerals like white-mica and chlorite.

On calculated norm compositions, Or increases seriously, Qtz increases slightly and Ab and An decrease. This is compatible with microscopic observations revealing that modal abundance of fine grained white-mica, epidote, microcline (and in a minor extent

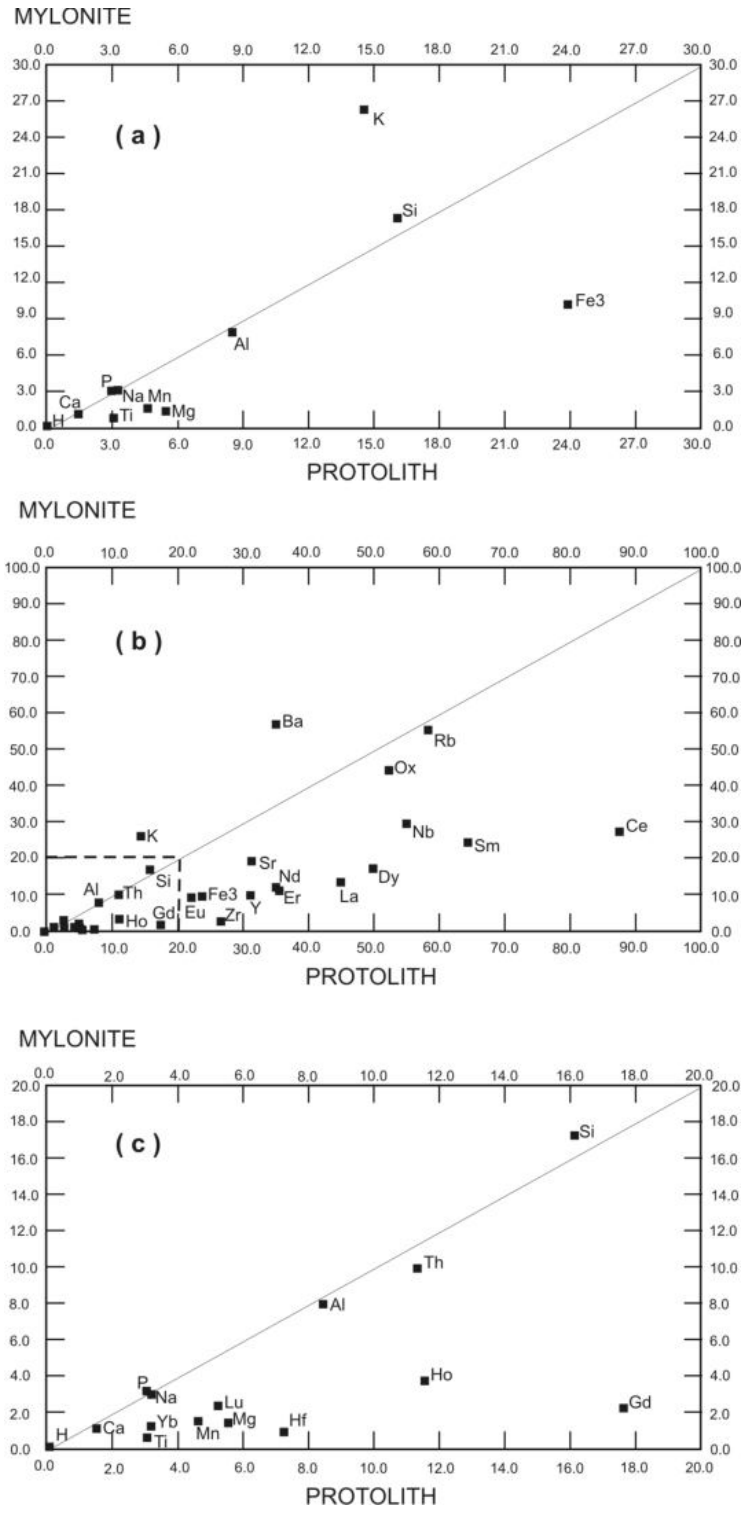

Figure 5: Isocon diagrams (constructed with the Gresens 92 code, Potdevin 1993) of representative ultramylonite (sample TM7-05) with respect to the protolith (sample TM1-05). El Tigre granitoid shear zone, Sierra de Pie de Palo, Western Sierras Pampeanas. (a) Plot of major elements as elements, (b) Plot of trace elements together major elements as elements and (c) corresponding close-up (dotted rectangular area in Fig. 5b). Scaling factors used to plot elements were: x100 for MnO and P_2O_5; x10 for MgO, K_2O, TiO_2, Dy, Er, Eu, Ho, Lu, Nd and Sm; x1 for Al_2O_3, CaO, Na_2O, Ce, Gd, Hf, La, Nb, Rb, Th, Y and Yb; x0.5 for SiO_2 and x0.1 for Ba, Sr and Zr.

TABLE 2: Whole-rock geochemistry of the ETG protolith and its mylonitic products, Sierra de Pie de Palo, Western Sierras Pampeanas. Major oxides expressed as weight percent, trace elements in ppm. Fe_2O_3 represents total Fe, nd: not determined.

	Undeformed/slightly deformed granitoid (protolith)					Moderately deformed granitoid			Proto mylo nite	Mylonite-Ultramylonite			
Sample/ Analysis	S4S	S15	S15S	S27	TM1-05	S21	TM3-05	TM6-05	TM4-05	S1S	T39	TM2-05	TM7-05
SiO_2	71.4	67.82	69.1	68.78	68.95	70.5	68.49	69.78	70.03	71.2	70.66	74.74	73.49
Al_2O_3	15.6	15.72	15.8	15.68	16.03	14.7	16.07	15.7	15.08	15.9	15.38	14.4	14.94
Fe_2O_3	2.58	3.46	2.61	2.7	3.42	2.98	3.84	2.9	2.89	2.42	2.03	1.05	1.44
CaO	2.39	2.28	2.39	1.98	2.19	1.72	2.17	2.41	2.08	1.76	1.43	1.1	1.5
MgO	0.81	0.91	0.89	0.71	0.92	0.77	0.89	0.71	0.76	0.8	0.48	0.16	0.22
Na_2O	4.79	3.64	4.25	3.82	4.3	3.61	3.73	3.55	3.83	4.48	3.74	4.19	4.03
K_2O	1.55	2.79	2.97	2.96	1.76	3.07	1.86	2.34	1.76	1.81	3.69	1.74	3.17
Cr_2O_3	nd	<0.01	nd	<0.01	<0.01	0.02	<0.01	<0.01	<0.01	nd	0.01	<0.01	<0.01
TiO_2	0.47	0.53	0.46	0.35	0.51	0.4	0.56	0.42	0.39	0.48	0.25	0.11	0.11
MnO	0.05	0.03	0.04	0.02	0.06	0.03	0.04	0.02	0.02	0.04	0.02	0.02	0.02
P_2O_5	0.10	0.11	0.12	0.10	0.07	0.07	0.07	0.09	0.10	0.08	0.07	0.08	0.07
SrO	nd	0.06	nd	0.05	0.04	0.03	0.04	0.04	0.04	nd	0.03	0.02	0.02
BaO	nd	0.16	nd	0.17	0.4	0.19	0.08	0.12	0.06	nd	0.13	0.05	0.07
LOI	0.4	0.91	1.25	0.89	0.65	1.01	1.1	1.01	1.2	1.4	0.81	0.86	0.69
TOTAL	100.4	98.42	99.88	98.21	98.94	99.1	98.94	99.09	98.24	100.4	98.73	98.25	99.77
Ba	820	1285	1770	1305	354	1505	643	982	496	1170	1035	400	567
Ce	nd	102	nd	66.3	87.5	103	78.7	98.3	93	nd	58.2	14.4	27.8
Co	nd	6.9	nd	5	7.4	4.5	5.2	5.	4.5	nd	2.5	4.9	3
Cr	nd	10	nd	<10	10	10	20	<10	<10	nd	<10	<10	<10
Cs	nd	1.5	nd	1.38	2.17	1.71	1.64	1.01	1.02	nd	0.56	0.46	0.59
Cu	nd	9	nd	<5	6	6	9	<5	5	nd	<5	<5	<5
Dy	nd	1.6	nd	1.26	5.02	1.62	3.09	2.9	4.36	nd	2.11	4.14	1.74
Er	nd	0.82	nd	0.63	3.57	0.72	1.8	1.49	2.09	nd	1	3.06	1.44
Eu	nd	1.02	nd	0.94	2.25	1	1.73	1.71	1.72	nd	0.97	1.53	0.97
Ga	nd	21.2	nd	19.4	17.7	18.6	18.6	17.8	17.6	nd	17.2	16.5	15.6
Gd	nd	3.85	nd	2.74	6.06	4.28	4.98	5.13	6.35	nd	3.42	3.61	2.16
Hf	nd	6.2	nd	5.6	7.3	6	6.8	5.9	7.6	nd	4.7	3.1	0.9
Ho	nd	0.32	nd	0.22	1.16	0.25	0.63	0.57	0.8	nd	0.38	0.99	0.37
La	nd	55.4	nd	36.5	45.2	54.6	42.4	52.2	46.8	nd	28.4	10.6	13.6
Lu	nd	0.18	nd	0.16	0.53	0.16	0.28	0.18	0.3	nd	0.16	0.55	0.23
Mo	nd	<2	nd	2	<2	<2	<2	<2	<2	nd	<2	<2	<2
Nb	21	4.5	19	4.3	5.5	5.7	6.4	5.7	6.4	5	5.1	2	2.9
Nd	nd	34.5	nd	23	35.6	37.1	31.5	36.1	37.4	nd	21.2	13.2	11.8
Pb	nd	41	nd	23	22	49	24	35	20	nd	27	19	24
Pr	nd	10.15	nd	6.78	9.57	10.75	8.58	10.15	10.2	nd	5.87	3.08	3.01
Rb	57	75.5	83	66.4	58.5	70.2	58.9	56.2	48.7	51	64.6	36.7	55.7
Sm	nd	5.06	nd	3.25	6.45	5.65	5.61	5.86	7.05	nd	3.83	2.96	2.47
Sr	446	430	568	356	316	264	311	319	300	381	231	183	197.5
Ta	nd	0.4	nd	0.4	0.3	0.4	0.5	0.4	0.4	nd	0.2	0.2	0.2
Tb	nd	0.42	nd	0.3	0.88	0.41	0.65	0.62	0.89	nd	0.45	0.62	0.29
Th	nd	13.45	nd	8.96	11.35	13	10.6	13.95	13.7	nd	11.45	0.96	9.94
Tm	nd	0.11	nd	0.09	0.52	0.09	0.26	0.18	0.32	nd	0.12	0.54	0.18
U	nd	2.99	nd	2.61	3.31	2.34	2.25	2.93	3.76	nd	1.97	3.19	0.99
V	nd	42	nd	32	46	33	53	51	37	nd	23	9	14
Y	9.01	8.3	15	6.1	31.5	7.3	16.8	16.4	22.3	44	11.4	35.2	10.4
Yb	nd	0.71	nd	0.6	3.19	0.66	1.61	1.16	1.76	nd	0.75	3.19	1.3
Zn	nd	173	nd	72	86	209	82	68	62	nd	55	24	36
Zr	491	236	262	205	269	233	254	227	274	296	163	78.8	27.74

quartz) increases, while plagioclase, biotite, garnet and accessory minerals decreases in the mylonites (Table 1).

Trace elements (including REE) are mostly depleted in higher mylonitized rocks except by Ba which shows an erratic behavior. The decreases in Ca and Sr (~ 41%) reflect the destruction of feldspar (plagioclase). Lower Y and Yb values have been observed in some deformed to highly deformed rocks when compared with representative sample of the protolith (sample TM1-05). The lower contents of these elements could be related with the lower garnet amount observed as deformation increases due the different deformational behavior with respect to the more plastic mica-rich matrix. Zr and Hf losses (~ 52% and ~ 54% respectively) could be related to the disappearance of abundant zircon present in the protolith. With respect to Zr, its behavior is quite different from that observed at Miéville, Switzerland, where granitic basement rocks of the Aiguilles Rouges Massif are cut by a shear zone generating a low-grade ultramylonite zone (Steyrer and Sturm 2002). Accessory zircon crystals from the Aiguilles Rouges undeformed granitoids and from the most highly deformed ultramylonites show only minor alterations and mechanical damage even in an extreme state of deformation. According to these authors, the outstanding stability of zircon allows considering the element Zr as immobile and therefore they use it as a passive marker for calculations of mass and volume changes during deformation.

Behavior of REE is less erratic. Chondrite normalized REE pattern (Fig. 6) shows high slope with $[La/Yb]_N$ = 9.48-55.32 and negative or absent europium anomaly (Eu/Eu* = 0.62-1.10). A slight decrease in the total REE amounts, but preserving a parallel pattern, is observed when compare normalized pattern of undeformed or slightly deformed El Tigre granitoid (sample TM1-05) with moderately and highly deformed ETG mylonite (samples TM3-05 and TM7-05, respectively). Similar behavior of REE has been observed in several mylonite zones (Condie and Sinha 1996, Czaplinski 2000). Although most of the

REE in the El Tigre granitoid reside in accessory phases such as garnet, monazite, allanite, apatite, rutile and zircon, the REE mobilization during mylonitization could be related with the decrease of modal garnet and accessory minerals in mylonites when compared with undeformed protolith. Disappearance of these accessory phases as has been confirmed in the petrographic study.

Although restricted SiO_2 mobilization, the occurrence of millimeter-wide quartz veinlets within the shear zone, implies removal of silica (considered as aqueous SiO_2) from the mylonites in an aqueous environment. This phenomenon can be related to enhanced solubility of strained quartz (Wintsch and Dunning 1985, Sinha *et al.* 1986).

Chemical changes in the El Tigre granitoid shear zone indicate that substantial removal and restricted addition of material has occurred due to fluid-rock interaction. The observed chemical variations are mostly controlled by syntectonic fluid-transport processes and features such as the disappearance of protolith minerals and the emergence of new phases.

Sr AND Nd ISOTOPIC VARIATIONS

To evaluate the effects of deformation on the isotopic systematic of the El Tigre granitoid, a Sr and Nd isotopic study was performed on three samples of progressively deformed rocks (samples TM1-05, TM3-05 and TM7-05). The Rb/Sr and Sm/Nd isotopic analyses were carried out on whole rock at the Geochronological Research Center, University of São Paulo, Brazil. The Rb-Sr and Sm-Nd analyses were prepared using the procedures of Tassinari *et al.* (1996) and Sato *et al.* (1995). Isotopic analyses of Sr and Nd were carried out on a multicollector VG 354 Micromass and Finnigan-MAT 262 mass spectrometers, respectively. Initial Sr and Nd isotopic ratios were calculated to an age of 1105 Ma, as deduced from U-Pb SHRIMP data (Morata *et al.* 2008).

High mobility has been detected in the Rb/Sr system meanwhile the Sm/Nd system seems to have a more closed behavior. It is notably to remark the high 87Sr/86Sr isotopic ratio measured in the ultramylonite when compared with the undeformed ETG.

TABLE 3: Analytical results of Rb-Sr and Sm-Nd isotopes from the El Tigre granitoid, Sierra de Pie de Palo, Western Sierras Pampeanas. eNdCHURt calculated using present-day values for a chondritic uniform reservoir (CHUR) of 147Sm/144Nd = 0.1967 and 143Nd/144Nd = 0.512638 (Jacobsen and Wasserburg 1984).

	Undeformed/slightly deformedprotolith (sample TM1-05)	Moderately deformed granitoid (sample TM3-05)	Highly deformed granitoid mylonite (sample TM7-05)
$(^{87}Sr/^{86}Sr)_0$	0.705425	0.698404	0.716548
$(^{143}Nd/^{144}Nd)_0$	0.5114236	0.5113322	0.5111604
εNd_{CHURt}	+4.15	+2.36	-1.0

As shown in Table 3, undeformed/slightly deformed granitoid (sample TM1-05) has an $(^{87}Sr/^{86}Sr)1105$ of 0.70543 and $(^{143}Nd/^{144}Nd)_{1105}$ of 0.511424, with εNd of +4.2. Moderately deformed ETG (sample TM3-05) evidences open system behavior mostly for the Sr isotopes during deformation, with $(^{87}Sr/^{86}Sr)1105 = 0.69840$, $(143Nd/144Nd)_{1105} = 0.511332$ and εNd of +2.4. Moreover, highly deformed ETG mylonite (sample TM7-05) has a more radiogenic signature $(^{87}Sr/^{86}Sr)_{1105} = 0.71655$, $(^{143}Nd/^{144}Nd)_{1105} = 0.511160$ and εNd of -1.0, which could be the consequence of high fluid-rock interaction between the granitoid and the host rocks during the mylonitization process. In fact, highly deformed granitoid (sample TM7-05) has the higher $^{147}Sm/^{144}Nd$ ratio and the lower Zr/Y ratio (≈ 2.2) compared with undeformed sample. Moreover, the different isotopic signature observed between the undeformed and mylonitized granitoid could be a consequence of mechanisms of deformation-driven processes assisted by fluid flow under open system conditions with different fluid-host rock interaction ratios.

DISCUSSION AND CONCLUSIONS

Mylonitic rocks were developed from a peraluminous garnet-bearing two mica granitoid (El Tigre Granitoid) as the result of strong ductile deformation restricted to narrow NEE oriented shear-zones (El Tigre granitoid shear zone), whose dextral shear sense is consistent with temporally and spatially related NNE striking regional ductile thrust along the western side of the Sierra de Pie de Palo.

Mylonitization provokes intense grain-size reduction, strong mylonitic foliation and stretching lineations development. Well preserved feldspar porphyroclasts are immersed in a very fine-grained quartz-phyllosilicate-epidote recrystallized matrix. Microstructures in these granitoid mylonites indicate that deformation occurred at low temperatures under greenschist facies retrogressive conditions. Microstructural analysis suggests the predominance of brittle and low-temperature plastic processes during mylonitic deformation.

Mylonitization at the El Tigre granitoid shear zone is also characterized by significant changes in modal and chemical composition denoting chemical breakdown. Retrogressed mineral assemblages found in the El Tigre granitoid mylonites, could imply the mobility of silica, enhanced permeabilities, solute transport during metamorphism and the requirement of fluids for metamorphic redistribution of elements (Sinha *et al.* 1986 and references therein).

Data here presented points to deformation-driven processes assisted by fluid flow (Yukiko *et al.* 2004). The chemical changes, coupled with the mineral assemblages observed in these mylonites, suggest that neoformed minerals are derived from the protolith assemblage by the addition of water and changes in the amounts of major and trace elements, and could be assigned

to a retrogressive event. Thus, the El Tigre granitoid shear zone had an apparent open-system behavior. Although it is very difficult to estimate the volume of fluid involved in this process, fluid content (determined as loss on ignition) shows an increasing of approximately 15% in the mylonites related to the protolith. Strain gradients shown by textural changes in minerals are accompanied by focused fluid flow through the mylonite zones where partial dynamic recrystallization under low-T conditions has occurred.

Based on petrographic observations, there are clear evidences that after igneous crystallization at 1105 Ma ± 4 Ma (U/Pb SHRIMP crystallization age on zircon from protolith, Morata *et al.* 2008), the ETG underwent regional amphibolite to greenschist facies metamorphism. Latter on time, the El Tigre granitoid experienced strong ductile deformation restricted to narrow mylonite zones and partial dynamic recrystallization under lower-T greenschists facies conditions, partly destroying and/or obliterating former relict igneous and regional metamorphic assemblages. Temperature conditions for this mylonitic stage could be assumed to have been in the order of 300-400 °C.

Recent $^{40}Ar/^{39}Ar$ hornblende crystallization ages of 515 ± 2 and 510 ± 3 Ma from amphibolite mylonite-ultramylonite of the Las Pirquitas thrust (Mulcahy *et al.* 2007) have been interpreted as the earliest phase of deformation during thrusting. The K/Ar age of 473 ± 10 Ma on very fine-grained recrystallized micaceous matrix from the El Tigre granitoid mylonite (Castro de Machuca *et al.* 2008) suggests that shearing in the Sierra de Pie de Palo occurred close to Early-Middle Ordovician during the Famatinian orogeny. This event was probably related to ductile thrusting and subsequent uplift during the initial terrane collision and prograde Famatinian metamorphism, defined as slightly before 460 Ma (Casquet *et al.* 2001). Mylonite zones with similar geometry of structures and kinematics were recognized elsewhere from the Sierra de Pie de Palo, suggesting that during the Famatinian orogeny the whole area was deformed under a similar shear regime and under similar thermal conditions.

ACKNOWLEDGEMENTS

The authors thank Dr. A. Guereschi and an anonymous reviewer for their constructive and helpful comments and suggestions. L. Previley is thanked for her help in the field work. Financial support for this research was provided by Project PIP 5649-CONICET (Argentina).

WORKS CITED IN THE TEXT

Astini, R., Benedetto, J. and Vaccari, N. 1995. The Early Paleozoic evolution of the Argentine Precordillera as a Laurentian rifted, drifted and collided terrane: a geodynamic model. Geological Society America Bulletin 107: 235-273.

Baldo, E., Casquet, C., Rapela, C., Pankhurst, R., Galindo, C., Fanning, C.M. and Saavedra, J. 2001. Ordovician metamorphism at the southwestern margin of Gondwana: P-T conditions and U-Pb SHRIMP ages from Loma de Las Chacras, Sierras Pampeanas. 3º South American Symposium on Isotope Geology, CD-ROM edition, 544-547, Pucón.

Casquet, C., Baldo, E., Pankhurst, R.J., Rapela C.W., Galindo, C., Fanning, C.M., and Saavedra J. 2001. Involvement of the Argentine Precordillera Terrane in the Famatinian Mobile Belt: geochronological (U-Pb SHRIMP) and metamorphic evidence from Sierra de Pie de Palo. Geology 29: 703-706.

Castro de Machuca, B. 1984. Geología del extremo sudoccidental de la Sierra de Pie de Palo, San Juan, República Argentina. PhD. Thesis, Facultad de Ciencias Exactas, Físicas y Naturales, Universidad Nacional de San Juan, unpublished, 187 p., San Juan.

Castro de Machuca, B., Arancibia, G., Previley, L., Pontoriero, S. and Morata, D. 2008. Ordovician mylonites from Mesoproterozoic granitoid, Sierra de Pie de Palo, Western Sierras Pampeanas, San Juan Province. 6º South American Symposium on Isotope Geology, CD-ROM edition, 4 p., San Carlos de Bariloche.

Condie, K. and Sinha, A. 1996. Rare earth and other trace element mobility during mylonitization: a comparison of the Brevard and Hope Valley shear zones in the Appalachian Mountains, USA. Journal of Metamorphic Geology 14(2): 213-226.

Czaplinski, W. 2000. Mobility of elements associated with deformation of the Izera Granite (Izera-Karkonosze Block, SW Poland). Goldschmidt 2000, Cambridge Publications, Journal of Conference Abstracts 5(2): 328.

Dalla Salda, L. and Varela, R. 1982. La estructura del basamento del tercio sur de la sierra de Pie de Palo, provincia de San Juan. 5º Congreso Latinoamericano de Geología, Actas 1: 451-468, Buenos Aires.

Finney, S., Gleason, J., Gehrels, G. and Peralta, S. 2003. Early Gondwanan connection for Argentine Precordillera. Earth Planetary Science Letter 205: 349-359.

Galindo, C., Casquet, C., Rapela, C., Pankhurst, R., Baldo, E. and Saavedra, J. 2004. Sr, C and O isotope geochemistry and stratigraphy of Precambrian and lower Paleozoic carbonate sequences from the Western Sierras Pampeanas of Argentina: tectonic implications. Precambrian Research 131: 55-71.

Grant, J.A. 1986. The isocon diagram- a simple solution to Gresens' equation for metasomatic alteration. Economic Geology 81: 1976-1982.

Jacobsen, S.B. and Wasserburg, G.J. 1984. Sm-Nd isotopic evolution of chondrites and achondrites. Earth and Planetary Science Letters 67: 137-150.

Morata D., Castro de Machuca, B., Previley, L., Pontoriero, S. and Arancibia, G. 2008. New evidence of Grenvillian crystalline basement in the Sierra de Pie de Palo, Western Sierras Pampeanas, Argentina: geotectonic implications. 6º South American Symposium on Isotope Geology, CD-ROM edition, 4 p., San Carlos de Bariloche.

Mulcahy, S.R., Roeske, S.M., McClelland, W.C. and Cain, J.C. 2004. The Las Pirquitas Thrust, a metamorphic high-strain zone of general shear. St. Catharines 2004 Technical Program, Abstract. Available on-line.

Mulcahy, S.R., Roeske, S.M., McClelland, W., Ellis, J.R., Nomade, S. and Vujovich, G. 2005. Timing and nature of forearc deformation and trenchward migration of the Famatina arc during accretion of the Precordillera Terrane. In Pankhurst, R. and Veiga, G. (eds.) Gondwana 12: Geological and Biological Heritage of Gondwana, Abstracts, Academia Nacional de Ciencias, p. 262. Córdoba.

Mulcahy, S., Roeske, S., McClelland, W., Nomade,

S. and Renne, P. 2007. Cambrian initiation of the Las Pirquitas thrust of the western Sierras Pampeanas, Argentina: Implications for the tectonic evolution of the proto-Andean margin of South America. Geology 35(5): 443-446.

Naipauer, M., Cingolani, C. A., McClelland, W. C., Vujovich, G. and Ellis, J. R. 2005. U-Pb (LA-ICP-MS) ages on detrital zircon grains from Angacos limestone siliciclastic levels (Caucete Group), San Juan province, Argentina: provenance implications for the Cuyania terrane. 5th South American Symposium on Isotope Geology, CD-ROM edition, Abstracts: 225-228, Punta del Este.

Nakamura, N. 1974. Determination of REE, Ba, Mg, Na and K in carbonaceous and ordinary chondrites. Geochimica et Cosmichimica Acta 38: 757-775.

Pankhurst, R.J. and Rapela, C.W. 1998. The proto-Andean margin of Gondwana: an introduction. In Pankhurst, R.J. and Rapela, C.W. (eds.) The Proto-Andean Margin of Gondwana, Geological Society, Special Publication 142: 1-9, London.

Passchier, C.W. and Trouw, R.A.J. 1996. Microtectonics. Springer, 189 p., Berlin.

Potdevin, J.L. 1993. Gresens92: A simple Macintosh program of the Gresens method. Computers & Geosciences 19(9): 1229-1238.

Ramos, V.A., Vujovich, G.I. and Dallmeyer, R.D. 1996. Los klippes y ventanas tectónicas preándicas de la Sierra de Pie de Palo (San Juan): edad e implicaciones tectónicas. 13º Congreso Geológico Argentino, Actas 5: 377-391, Buenos Aires.

Ramos, V.A., Dallmeyer, D. and Vujovich, G.I. 1998. Ar/Ar constraints in the age of deformation of the Pie de Palo basement: implications for the docking of Precordillera and Chilenia. In Pankhurst, R.J. and Rapela, C.W. (eds.) The Proto-Andean margin of Gondwana. Geological Society, Special Publication 142: 143-158, London.

Ramos, V. and Vujovich, G. 2000. Hoja Geológica 3169-IV San Juan, provincia de San Juan. Boletín Nº 243, Servicio Geológico Minero Argentino, 82 p., Buenos Aires.

Rapela, C., Pankhurst, R., Baldo, E., Casquet, C., Galindo, C., Fanning, C. M. and Saavedra, J. 2001. Ordovician metamorphism in the Sierras Pampeanas: new U-Pb SHRIMP ages in central-east Valle Fértil and the Velazco batholith. 3º South American Symposium on Isotope Geology, CD-ROM edition, 616-619, Pucón.

Sato, K., Tassinari, C.G.C., Kawashita, K. and Petronillo, L. 1995. O método geocronológico Sm-Nd no IG-USP e suas aplicações. Anais da Academia Brasileira de Ciências 67: 313-336.

Sinha, A. K., Hewitt, D.A. and Rimstidt, J.D. 1986. Fluid interaction and element mobility in the development of ultramylonites. Geology 14: 883-886.

Steyrer, H.P. and Sturm, R. 2002. Stability of zircon in a low-grade ultramylonite and its utility for chemical mass balancing: the shear zone at Miéville, Switzerland. Chemical Geology 187(1-2): 1-19.

Tassinari, C.C.G., Medina, J.G.C. and Pinto, M.C.S. 1996. Rb-Sr and Sm-Nd Geochronology and Isotope Geochemistry of Central Iberian Metassedimentary Rocks (Portugal). Geologie en Mijnbouw 75: 69-79.

Thomas W.A. and Astini, R.A. 1996. The Argentine Precordillera: a traveler from Ouachita embayment of North America Laurentia. Science 273: 752-757.

Vujovich, G. and Ramos, V. 1994. La faja de Angaco y su relación con las Sierras Pampeanas Occidentales. 7º Congreso Geológico Chileno, Actas 1: 215-219, Concepción.

Vujovich, G., van Staa1, C. R. and Davis, W. 2004. Age Constraints on the Tectonic Evolution and Provenance of the Pie de Palo Complex, Cuyania Composite Terrane, and the Famatinian Orogeny in the Sierra de Pie de Palo, San Juan, Argentina. Gondwana Research 7(4): 1041-1056.

Wintsch, R.P. and Dunning, J. 1985. The effect of dislocation density on the aqueous solubility of quartz and some geological implications: a theoretical approach. Journal of Geophysical Research 90 (B5): 3649-3658.

Yukiko, O., Hisae, S. and Masao, B. 2004. Chemical changes of an ultramylonite band - a case of the Futaba shear zone. 32nd International Geological Congress, CD-ROM edition, Abstracts. Florence.

Recibido: 4 de noviembre, 2009
Aceptado: 7 de diciembre, 2009